Development and experimental validation of an analytical model to predict the demoulding force in hot embossing

2014 J. Micromech. Microeng. 24 055007

(http://iopscience.iop.org/0960-1317/24/5/055007)

OPEN ACCESS
IOP Publishing
Made open access 4 June 2014
Journal of Micromechanics and Microengineering
J. Micromech. Microeng. **24** (2014) 055007 (11pp)
doi:10.1088/0960-1317/24/5/055007

Development and experimental validation of an analytical model to predict the demoulding force in hot embossing

F Omar[1], **E Brousseau**[1], **A Elkaseer**[1,2], **A Kolew**[3], **P Prokopovich**[1,4] **and S Dimov**[5]

[1] Cardiff School of Engineering, Cardiff University, Cardiff, UK
[2] Production Engineering and Mechanical Design Department, Faculty of Engineering, Port Said University, Port Said, Egypt
[3] Karlsruhe Institute of Technology, Karlsruhe, Germany
[4] Cardiff School of Pharmacy and Pharmaceutical Sciences, Cardiff University, Cardiff, UK
[5] School of Mechanical Engineering, University of Birmingham, Birmingham, UK

E-mail: BrousseauE@cf.ac.uk

Received 16 May 2013, revised 2 February 2014
Accepted for publication 6 March 2014
Published 3 April 2014

Abstract

During the demoulding stage of the hot embossing process, the force required to separate a polymer part from the mould should be minimized to avoid the generation of structural defects for the produced micro structures. However, the demoulding force is dependent on a number of process factors, which include the material properties, the demoulding temperature, the polymer pressure history and the design of the mould structures. In particular, these factors affect the chemical, physical and mechanical interactions between a polymer and the replication master during demoulding. The focus of the reported research is on the development and validation of an analytical model that takes into account the adhesion, friction and deformation phenomena to predict the required demoulding force in hot embossing under different processing conditions. The results indicate that the model predictions agree well with the experimental data obtained and confirm that the design of the mould affects the resulting demoulding force. In addition, the applied embossing load was observed to have a significant effect on demoulding. More specifically, the increase in pressure within the polymer raises the adhesion force while it also reduces the friction force due to the decrease in the thermal stress.

Keywords: hot embossing, demoulding, PMMA

(Some figures may appear in colour only in the online journal)

1. Introduction

Fabrication processes for the high volume production of parts with micro and nano scale features are very important in the global research and industry efforts to meet the increasing needs for device miniaturization in numerous application areas (Hansen *et al* 2011). Micro injection moulding (Griffiths *et al* 2011), hot embossing (HE) (Worgull 2009) and UV nanoimprint lithography (Haisma *et al* 1996) are proven replication technologies for large series production of polymer parts with micro and nano scale structures. Among these replication technologies, HE is a process which relies on raising the temperature of a sheet of polymer and then on pressing a heated master plate into the polymer for triggering a local flow of the material to fill and replicate surface structures. More specifically, an embossing cycle starts by bringing the mould and the substrate plates closer to each other until an initial contact between the polymer and the mould generates a force of around 100 to 300 N. Then, the material to be replicated and the mould are heated above the glass transition temperature for amorphous polymers or up to the melting range for semi-crystalline polymers. Following

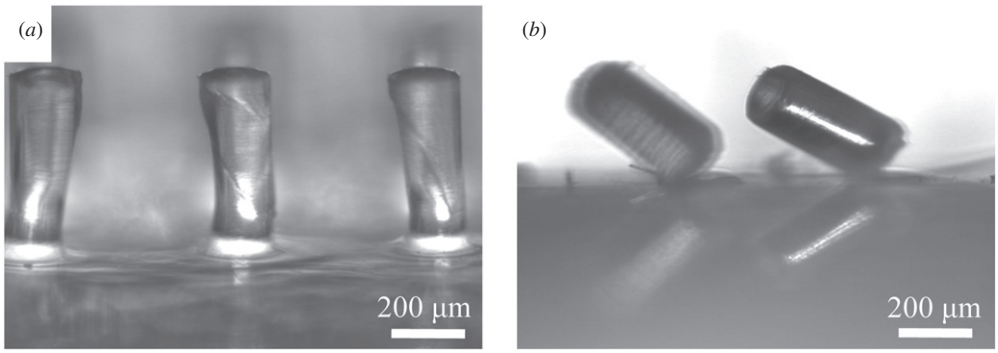

Figure 1. Examples of demoulding defects: (*a*) overstretched features (10% elongation) (*b*) broken structures.

this step, the polymer and mould are further pressed together until a set force is attained; this stage is referred to as velocity-controlled moulding. Then, the process switches to a force-controlled moulding mode during which the embossing force is kept constant for a duration determined by the holding time. Next, the cooling cycle starts. This cycle is characterized by the reduction of the embossing temperature until a set demoulding temperature is reached while maintaining the applied embossing force. Finally, the embossed polymer is separated from the mould by moving the plates away from each other. HE enables relatively high aspect ratio features to be replicated while their sizes can vary from several hundred micrometres down to several nanometres. This technology has attracted a significant interest in recent years, in particular due to the relatively simple set-ups and short lead times associated with its implementation in comparison to other replication processes.

Although the polymer replication techniques mentioned above are suitable for the production of parts with micro and nano structures, one of the most challenging issues to overcome when implementing them is to prevent the formation of structural defects that can occur during demoulding. In the case of hot embossing, such problems have been reported by a number of researchers (Worgull and Heckele 2004, He *et al* 2005, Dirckx *et al* 2007, Guo *et al* 2007a, Dirckx and Hardt 2011). Demoulding-related defects can include overdrawn or damaged edges due to thermal stresses associated with differences in the shrinkage behaviour of replicas and the mould during cooling, and overstretched and separated structures, such as those depicted in figure 1, due to high adhesion and friction forces. For instance, overdrawn or damaged edges are problematic for the production of microfluidic systems as they can affect the sealing between cover plates and channels of the HE replicas, and also can compromise the functionality of the fabricated devices. In addition, broken or overstretched features can render the HE replicas unusable and can result in polymer material residue in the mould cavities, which is also detrimental in batch production of parts. Another costly defect, which is sometimes reported in the literature, consists of broken mould structures/features (Dirckx 2010).

Reported experimental studies on demoulding in hot embossing refer to qualitative (Dirckx *et al* 2007, Hirai *et al* 2003) and quantitative (Trabadelo *et al* 2008, Park *et al* 2009) evaluations of the effect of the demoulding temperature or that of including additional mould structures. These studies generally reveal that the demoulding force initially decreases with the reduction of the demoulding temperature and then, when a given minimum value is reached, it starts increasing as the temperature is further decreased. However, limited demoulding temperature ranges are commonly considered and only a single type of HE mould design is generally tested in such studies. In one particular paper, Worgull *et al* (2008a) described a specialized test apparatus used to characterize the friction between embossed polymers and mould materials. It was reported that variations of embossing temperatures and pressures influenced the static friction coefficient, while the dynamic friction coefficient was affected by the mould material and its surface roughness.

The majority of the theoretical investigations of the demoulding stage in hot embossing polymer microstructures includes finite element (FE) simulations of demoulding forces that consider the effects of thermal stresses and sidewall friction between the replica and the mould (He *et al* 2005, Worgull *et al* 2005, Worgull *et al* 2008b, Song *et al* 2008, Hsueh *et al* 2006). In particular, these simulations were used to study the effect of sidewall friction on the stresses in the parts and mould or on the demoulding forces. In addition to the thermal stress and the sidewall friction, Guo *et al* (2007b) and Dirckx and Hardt (2011) considered the contribution of the adhesion force between the replica and the mould in creating their FE models. The latter authors also implemented a special test method that was similar to the cantilever beam fracture technique in order to study the effect of feature geometry and demoulding temperature on the demoulding toughness, which corresponds to the energy dissipated during the separation of the part from the mould. Although, the replica-plate separation method studied was not representative of the typical demoulding technique used in commercial HE machines, it provides valuable information about adhesion and friction dominated demoulding phenomena.

The literature review reveals that, while the developed FE models contribute to a better understanding of the demoulding process mechanisms in HE, there is still a need to develop more comprehensive simulation models for investigating the combined effects of material properties, demoulding temperatures, polymer pressure histories, locations and geometry of the mould structures and the adhesion on the

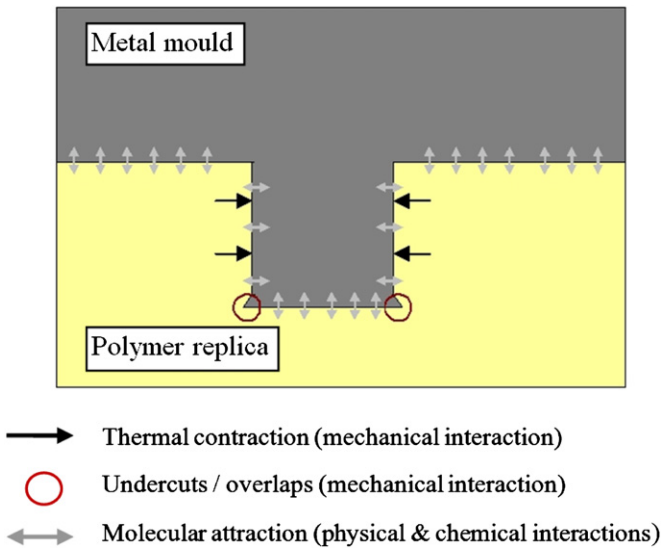

Figure 2. Schematic of mechanisms affecting demoulding.

demoulding forces. In this context, the motivation for the research presented in this paper is to develop and validate an analytical model for predicting the demoulding force in hot embossing of polymer materials by taking into account these process factors. An analytical approach was preferred over the development of an FE solution in order to reduce the computational complexity generally associated with FE models. In addition, the ultimate aim of the developed model is to support subsequent studies targeted at optimizing the demoulding step of the HE process to reduce structural defects in replicas. So far, the existing FE models have had a relatively limited application as tools for optimizing this process step.

2. Factors affecting demoulding

A comprehensive understanding of the mechanisms involved in the demoulding of polymer parts is a complex task as several factors of different nature influence this process. More specifically, the required separation force is dependent on chemical, physical and mechanical interactions between replicas and plates as illustrated in figure 2.

The physical and chemical interactions are responsible for the adhesion of replicas to the plates. In particular, adhesion is the result of molecular attraction that holds the surfaces of two dissimilar substances together (Gerberich and Cordill 2006). Chemical interactions comprise covalent bonds, ionic or electrostatic bonds, and metallic bonds. Physical interactions include hydrogen and van der Waals bonds as a result of intermolecular forces. Hydrogen and van der Waals bonds are much weaker than the chemical interactions as they do not involve electron exchange. Van der Waals forces are always present when two asperities are in close proximity. Metals, which have relatively little attraction for their valence electrons, tend to form ionic bonds when they interact with non-metals. If a polymer is brought into contact with a metal, there is a large separation of charge at the interface. This results in an electrostatic attraction between them in addition to the van der Waals interaction (Bhushan 2003). Moreover, adhesion affects friction forces; the so-called adhesive friction is the effort required to break the cold-welded junctions between asperity pairs on contiguous surfaces (Prokopovich *et al* 2010).

It was observed by Dirckx (2010) that a decrease of the demoulding temperature reduces the contribution of the adhesion force significantly until a point where the demoulding force becomes dominated by friction. Other studies also showed that mould and polymer materials have an effect on the adhesion phenomena (Guo *et al* 2007a, Saha *et al* 2010, Jaszewski *et al* 1999, Park *et al* 2004). For instance, the application of coatings on the mould surface can improve the demoulding in HE as it reduces the influence of the chemical and physical interactions.

The contribution of mechanical interactions to the demoulding force manifests itself on the sidewalls of the mould structures and it is a consequence of (1) friction and (2) interlocking of undercut features. In this study, such interlocking is considered to be the result of the surface waviness inherent to the mould machining process utilized. The effect of friction is measured by the coefficient of friction which is the ratio of the friction force to the normal force acting on the contact area. In the case of HE, the normal force is caused by the difference in the shrinkage between the mould and the polymer material as well as by the adhesion force, whose influence is typically smaller than the thermal stress and thus could be neglected in some cases. As polymers have higher shrinkage rates than metals, this leads to a high contact stress between the mould and the polymer on the sidewalls of the structures to be replicated (Dirckx *et al* 2007, Guo *et al* 2007b, Titomanlio and Jansen 1996). Previous studies also suggested that undercuts or overlaps could restrain the material into the mould and cause further deformations or failures during demoulding. For example, investigations conducted by Pham and Colton (2002) and Delaney *et al* (2010) showed that, for moulds fabricated by stereolithography (SLA) or turning, the resulting surface waviness, or stair-step topography in the case of SLA, on the sidewalls increases the demoulding force as such surface features act as undercuts. It was also observed that moulds with structures that incorporate a draft angle such as silicon moulds produced by potassium hydroxide (KOH) etching could be demoulded more easily (Esch *et al* 2003). This further suggests that the influence of such mechanical interactions should not be neglected during the demoulding process.

3. Model development

The model was developed to consider the combined effects of friction, deformation and adhesion phenomena. Thus, the demoulding force, F_d, is constituted of the following three components: (1) the adhesion force between the mould and the polymer, F_{ad}, (2) the deformation force, F_{def}, due to the presence of undercuts on the sidewalls of the mould structures, which are inherent to master making processes and (3), the friction force on the structure sidewalls, F_{fr}:

$$F_d = F_{ad} + F_{\text{def}} + F_{fr}. \quad (1)$$

It should be noted that the adhesion force, F_{ad}, is considered explicitly only for the horizontal surfaces of the

mould. The adhesion between the vertical sidewalls and the polymer is comprised in the friction force, F_{fr}.

3.1. Adhesion force

The detailed calculation of the adhesion force is difficult because adhesion is a function of the material pair properties and interface conditions such as crystal structure, crystallographic orientation, solubility of one material into another, chemical activity, surface cleanliness, normal load, temperature, duration of contact and separation rate (Bhushan 2003). A simplified approach for modelling adhesion uses the concept of surface energy. In particular, this energy contributes to the work of adhesion, W_{ad}, for which the surface energies of the two solids, separately, and the interfacial energy between the two materials in contact are considered. Fundamental adhesion models such as the JKR (Johnson *et al* 1971) or DMT (Derjaguin *et al* 1975) models incorporate W_{ad} to predict the adhesion force between two solids. A recent review provides a comprehensive description of different adhesion models available to date (Prokopovich and Starov 2011). The application of fundamental adhesion models in the context of this study requires the calculation of the work of adhesion between the mould and the polymer for different demoulding temperatures. However, this task is hampered by the lack of theoretical and experimental data in the temperature range of interest. For this reason, a model proposed by Kendall (1973) which describes the adhesion strength change of a material with temperature variations is applied to predict the adhesion force at different demoulding temperatures for the HE process. This model considers that the residual stress due to the shrinkage of the material contributes to the strain energy of the system, which in turn reduces the initial adhesive energy required to fracture a unit area interface at zero shrinkage, γ:

$$\sigma_{ad} = \left[\frac{2K}{t_p}\left(\gamma - \frac{t_p.K\varepsilon^2}{2}\right)\right]^{1/2} \tag{2}$$

where σ_{ad} is the adhesion strength, ε is the thermal shrinkage strain, which is equal to the coefficient of thermal expansion of the polymer, α_p, multiplied by the change in temperature considered, ΔT, t_p is the thickness of the polymer and K is the bulk modulus, which is expressed as follows:

$$K = \frac{E}{3(1-2\nu)} \tag{3}$$

where ν is the Poisson ratio and E is the Young's modulus of the polymer. Thus, the expression of the adhesion force adopted in this study is as follows:

$$F_{ad} = \sigma_{ad} \times A \tag{4}$$

where A is the total horizontal surface area of contact between the polymer and the mould.

3.2. Deformation force

Metal replication masters are often structured by mechanical processes. Thus, the machined surfaces have a specific waviness profile that can cause interlocking on the sidewalls of the mould features leading to demoulding issues. In particular, the polymer replica has to deform to slide over the master during demoulding at locations where interlocking occurs. Colton *et al* (2001) proposed a model to predict the ejection force in injection moulding, which takes into account the waviness of periodic surfaces and implemented it for moulds fabricated with the stereolithography process (Pham and Colton 2002). This model was also recently adapted by Delaney *et al* (2010) and applied to surfaces machined by turning. Colton's model introduces an 'equivalent' coefficient of friction, which is the sum of the coefficient of friction and a contribution from the elastic deformations of the mould and the polymer parts that are necessary to overcome the interlocking between them due to the periodic waviness profile on the sidewalls of the mould structures.

In this study, the mould cavities are created with micro drilling and thus, the generated surface on the sidewalls of such features is also periodic. For this reason, the model from Colton *et al* (2001) was adapted to describe the deformation force F_{def} as follows:

$$F_{def} = \frac{\delta^2}{l \times r_c} \cdot \frac{E}{1-\nu} \cdot A_w \tag{5}$$

where δ represents the maximum peak to valley distance generated with the micro drill, l and r_c are the tooth load and the tool nose radius respectively, E and ν are the Young's modulus and the Poisson ratio of the polymer and A_w is the area of contact on the sidewalls of the cavities. Given that the feed rate, f, spindle speed, V, and tool nose radius used during the micro drilling process are known parameters, it is possible to calculate δ as follows (Elkaseer *et al* 2012):

$$\delta = r_c - \sqrt{r_c^2 - \left(\frac{f}{2}\right)^2} \tag{6}$$

In addition, l can also be expressed as:

$$l = \frac{f}{n \times V} \tag{7}$$

where n is the number of teeth of the micro drill.

3.3. Friction force

The force required during demoulding must overcome the effect of the normal forces on the sidewall of the micro structures present in the mould. Most mathematical models developed to quantify the demoulding process simply derive the expression of the friction force based on the empirical Coulomb's law of friction (Menges and Mohren 1986). Thus, in this study the friction force, F_{fr}, is described by:

$$F_{fr} = \mu \cdot \sigma_d \cdot A_w \tag{8}$$

where μ is the coefficient of friction, σ_d is the contact stress on the sidewalls of the mould structures upon demoulding and A_w is the area of contact between the polymer and the mould on the sidewalls. The contact stress, σ_d, should be considered based on two different HE processing stages, namely during cooling and upon demoulding, in order to take into account the polymer pressure history.

To achieve this, the contact stress upon demoulding is examined first. In particular, when demoulding begins, the mould does not exert any pressure on the polymer and thus, the stress that results from the shrinkage behaviour of the polymer

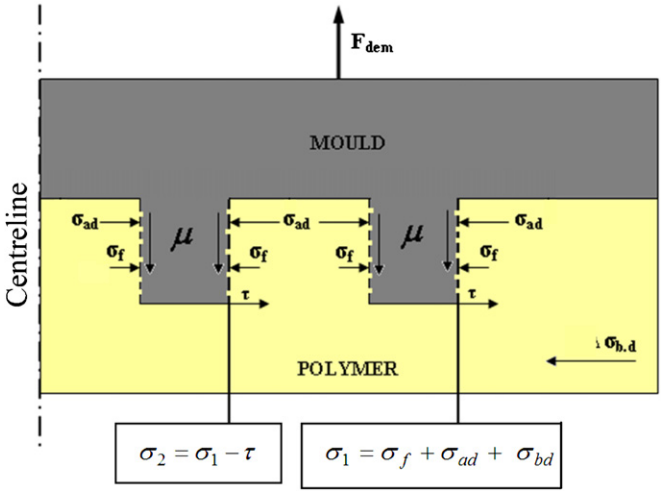

Figure 3. Contact stress upon demoulding.

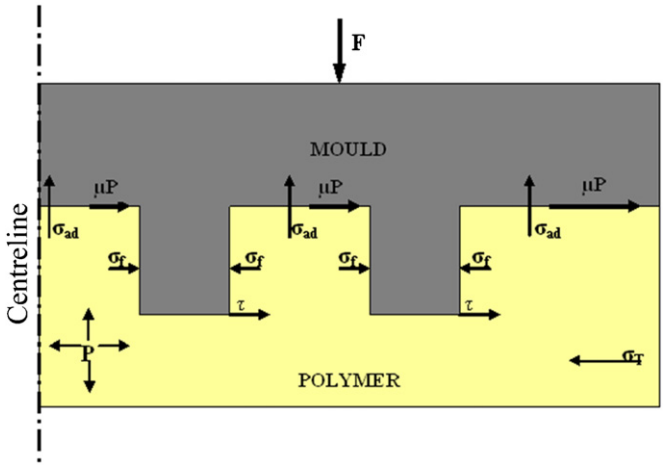

Figure 4. Contact stress before demoulding.

as it is cooled down, tends to move towards the centre of the replica. In this case, the stress condition within the polymer is illustrated in figure 3 and the contact stress upon demoulding is expressed as:

$$\sigma_d = \sigma_f + \sigma_{ad} + \sigma_{bd} \tag{9}$$

where σ_{ad} is described by (2) and manifests itself on the vertical walls as illustrated in figure 3, σ_{bd} is the contact stress before demoulding and σ_f is the flow-induced residual stress. The flow-induced residual stress, σ_f, can be explained as follows. When a polymer is in a molten state, its molecules are unstressed and they tend to reach an equilibrium state. During HE, the polymer is sheared and elongated and as a result, the molecules are oriented in the flow direction. If the polymer solidification occurs before the molecules can fully relax back to their state of equilibrium, the molecular orientation is locked within the embossed replica and this creates such type of stress. However, to simplify the development of the proposed model, σ_f is not considered in this study.

As shown in figure 3, the contact stress on a given mould structure is also dependent on its location. This is due to the fact that the polymer is also subjected to shear stress, τ, which occurs as the polymer shrinkage towards the centre of the replica is prevented by the mould surface structures/features. This is the reason why additional structures are sometimes incorporated in the margin region of the HE plates in order to absorb most of the stress and thus, to reduce the risk of damage to some functional features during the replication process (Worgull 2009). This shear stress can be expressed as follows:

$$\tau = \frac{F_{bd}}{A_s} \tag{10}$$

where A_s is the area of the surface at the open end of a given mould structure where the normal vector to this surface is orthogonal to the shrinkage direction and F_{bd} is the force generated by σ_{bd}. More specifically, F_{bd} is the product between σ_{bd} and an area having a width defined by the cross section of a microstructure and a height by the distance between the bottom of the polymer and the mould. In figure 3, σ_1 represents the contact stress upon demoulding on the mould feature which is further away from the replica centre and it is calculated using equation (9). Then, the contact stress, σ_2, acting on the adjacent structure in the lateral direction towards the core of the polymer is derived from σ_1 by taking into account the influence of the shear stress, τ, and is given by:

$$\sigma_2 = \sigma_1 - \tau. \tag{11}$$

In this way, the contact stress upon demoulding can be calculated as a function of the mould design, in particular by considering the location of the mould structures. However, in order to express σ_d using equation (9) above, the contact stress before demoulding, σ_{bd}, should be calculated. For this, the distribution of σ_{bd} when the polymer is cooled down to the demoulding temperature while it is still subjected to the embossing load is illustrated with figure 4. From the figure, it can be seen that the friction, adhesion and pressure within the replica tend to oppose thermal shrinkage towards the centre of the replica. Thus, to account for the reduced shrinkage effect due to these factors, σ_{bd} is expressed with the following equation:

$$\sigma_{bd} = \sigma_T - (P + \mu(P + \sigma_{ad})) \tag{12}$$

where σ_T is the thermally-induced residual stress, P is the pressure generated due to the applied force while $\mu\sigma_{ad}$ is acting on the horizontal surfaces. P shows a parabolic distribution in open die embossing due to the polymer flow and can be calculated with (Lin *et al* 2003):

$$P = \frac{n+3}{n+1}\left[1 - \left(\frac{r}{R}\right)^{n+1}\right]\frac{F}{A} \tag{13}$$

where F is the applied force, R is the overall radius of the polymer sheet after embossing and r is the radius at a given point, n is the material constant and in the case of PMMA, $n = 0.25$ (Lin *et al* 2003). It should be noted that this pressure distribution is not valid when the lateral flow of the polymer melt is prevented using special fixtures.

The thermally-induced residual stress, σ_T, arises during the cooling stage and is a consequence of polymer shrinkage. In particular, the thermal expansion of polymers is significantly higher than that of metals. Thus, this difference in thermal shrinkage during cooling results in high contact stress between a replica and a metallic master which, in turn, contributes to

the demoulding force. The influence of this phenomenon is therefore important for all replication processes, especially when the feature size decreases. The thermally-induced residual stress is expressed as follows:

$$\sigma_T = (\alpha_p - \alpha_m)(T_g - T_d)\frac{E}{1-v} \tag{14}$$

where: α_p and α_m are the coefficients of thermal expansion for the polymer and the mould material respectively, T_d is the demoulding temperature for the replica and T_g denotes the solidification temperature which corresponds to the glass transition temperature for amorphous thermoplastics or the melting temperature for semi crystalline polymers.

3.4. Modelling assumptions

In practice, the following factors also contribute to the demoulding force. However, in this study, they were not included in the model and thus kept constant in the validation experiments:

- Embossing temperature: a higher embossing temperature contributes to a better filling of intricate surface features, which results in increased interlocking. This interlocking is reflected by an increased demoulding force. Initial experiments conducted by the authors at different temperatures (120, 150 and 180 °C) indicated that extremely high demoulding forces could be observed at high embossing temperatures while poor filling was detected at low temperatures.
- Holding time: during the velocity-controlled moulding stage of the process, the pressure gradient increases and reaches a maximum at the end of this moulding step. After switching to force-controlled moulding, the pressure gradient decreases with time as the moulded area increases due to the creeping of the melt under constant load. Former simulation studies indicate that, at the end of a holding time of 280 s, the maximum pressure decreases by about 57% for PMMA (Worgull 2009). The model used for the prediction of the demoulding force in this research does not consider the creep time effect. Therefore, the pressure distribution within the polymer is considered constant with time.
- Demoulding speed: initial experiments carried out by the authors revealed that the demoulding speed has an influence on the demoulding force. Three different velocities, namely 0.5, 1 and 5 mm min^{-1} were selected for these initial trials. It was not possible to record any demoulding force at 5 mm min^{-1} due to the limited resolution of the force sensor used. At lower velocity of 0.5 mm min^{-1}, it was also difficult to detect any clear demoulding force signal in the force curve history, which was an indication that demoulding happened as a peeling movement in this case.
- Stress variation in the vertical direction: previous FE studies showed that there is a variation of stress in the vertical direction (Guo *et al* 2007b). In this research however, it is assumed that no stress variations occur in the vertical direction.

Table 1. PMMA material properties.

Properties	Symbol	Values
Young's modulus (50 °C)	E	2.42 GPa
Young's modulus (60 °C)		2.15 GPa
Young's modulus (70 °C)		1.88 GPa
Young's modulus (80 °C)		1.61 GPa
Young's modulus (90 °C)		1.34 GPa
Coefficient of friction	μ	0.4
Poisson ratio	v	0.39
Glass transition temperature	T_g	105 °C
Coeff of thermal expansion	α_p	8.4×10^{-5}/°C

In addition, the following assumptions were also made in the particular implementation of the model, which is described in the following sections.

- When estimating the friction force, the surface of contact, A_w, between the polymer and the sidewalls of the micro structures present in the mould is considered to be the complete vertical area of such features. This surface of contact is influenced by the shrinkage of the polymer and in reality, it is not trivial to define its exact area where the different stress components are at play.
- The adhesion strength on the vertical walls of the mould features is assumed to be the same as that present on the horizontal surface of the mould. It is considered that this approximation does not bring a significant error to the calculations in situations where the surface area along the vertical walls is very small compared to the surface area along the horizontal mould surface, which is the case of the implementation reported in this study.

4. Experimental set-up

Experiments were conducted with an HEX03 HE machine from Jenoptik Mikrotechnik to validate the proposed model. The following sub-sections describe the design and the manufacture of the mould used along with the properties of the polymer material processed, the experimental design adopted and the measurement technique employed to assess the demoulding force. The mould design, the polymer properties and the experimental plan were also used as an input for the conducted simulation study in order to compare the theoretical and experimental results.

4.1. Test material and mould design

Two millimetre thick PMMA sheets were used in the experiments. PMMA is an amorphous polymer and one of the common choices for HE. The PMMA mechanical and thermal properties are shown in table 1. The Young's modulus values for PMMA are given at the different temperatures which are of interest for the experiments conducted in this research. They are taken from Dirckx (2010).

The embossing mould was made from a 5 mm thick aluminium workpiece with overall lateral dimensions of 40 mm × 40 mm. The material properties of the aluminium used to produce the test plate are given in table 2. The

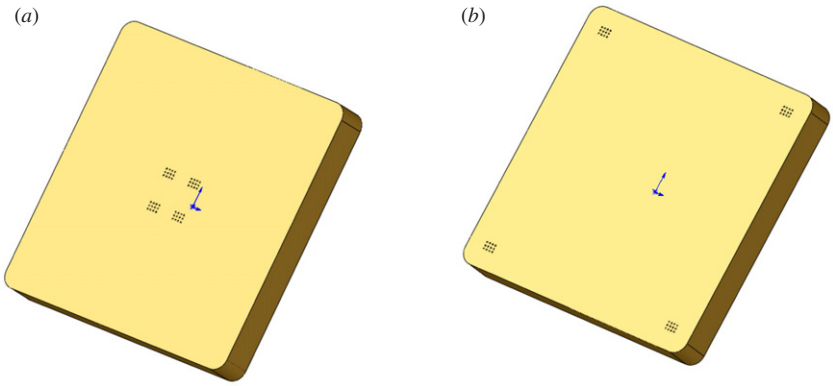

Figure 5. Mould design: structures located in (*a*) the central area and (*b*) the corners.

Table 2. Aluminium material properties.

Properties	Symbol	Values
Young's modulus	E	70 GPa
Poisson ratio	ν	0.33
Coeff. of thermal expansion	α_m	$2.4 \times 10^{-5}/^{\circ}\mathrm{C}$

Table 3. Micro drilling parameters.

Parameters	Symbol	Values
Feed rate	f	77 mm min^{-1}
Spindle speed	V	18 000 rev min^{-1}
Tool number of teeth	n	2
Tool nose radius	r_c	5 μm

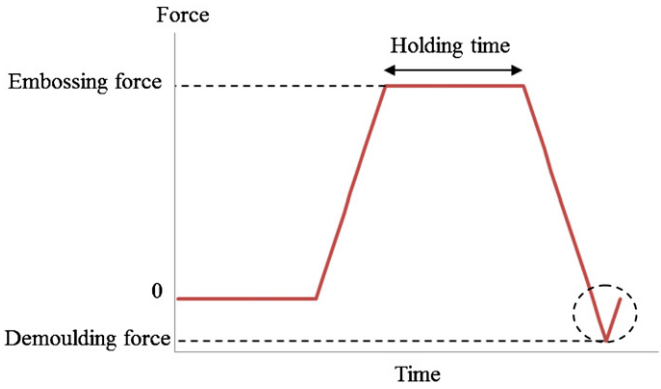

Figure 6. Typical force evolution during the HE process.

Table 4. Experimental design.

Trial	F (kN)	T_{dem} (°C)
1	15	90
2	15	80
3	15	70
4	15	60
5	15	50
6	5	90
7	5	50
8	25	90
9	25	50

structured area of the mould includes four arrays of 3 × 4 micro drilled holes. The depth of each hole was 400 μm and the diameter 200 μm. To assess the effect of the holes' location on the demoulding force, two designs were implemented. For the first design, the four arrays of holes were positioned in the central area of the mould while, for the second design, an array of holes was located at each corner of the aluminium workpiece.

The holes were produced by micro drilling on a Kern HSPC 2216 machining centre. The machining parameters utilized during the drilling process are given in table 3. The respective designs of the moulds are given in figure 5.

4.2. Planning of experiments and force measurements

In these experiments, the demoulding force was measured as a function of the demoulding temperature, T_{dem}, when varying it in the range from 50 to 90 °C. In addition, measurements were also conducted when varying the applied embossing force, F, at the maximum and minimum values considered for T_{dem}. For all trials, the embossing temperature was kept at 150 °C, while the holding time was 1 min and the demoulding velocity applied was 1 mm min^{-1}. Each of the trials was repeated three times. The combinations of the parameters' values utilized for F and T_{dem} are provided in table 4. The chosen range of parameters levels was determined based on material properties and preliminary experiments in order to ensure complete filling of the mould cavities during the embossing stage of the process and also to study an extended range of demoulding temperatures.

The demoulding force required in each experiment was measured with the force sensor built into the hot embossing machine. The output of the sensor provides online force curves in which the demoulding force is characterized by a sudden release of the mould from the polymer leading to characteristic 'jumps' as illustrated in figure 6. In this research, the master was fixed onto the top plate of the HE machine using screws. In addition, the bottom plate was sand blasted prior to the experiments as recommended by Worgull (2009) in order to ensure that demoulding occurs between the mould and the replica and not between the bottom plate and the replica.

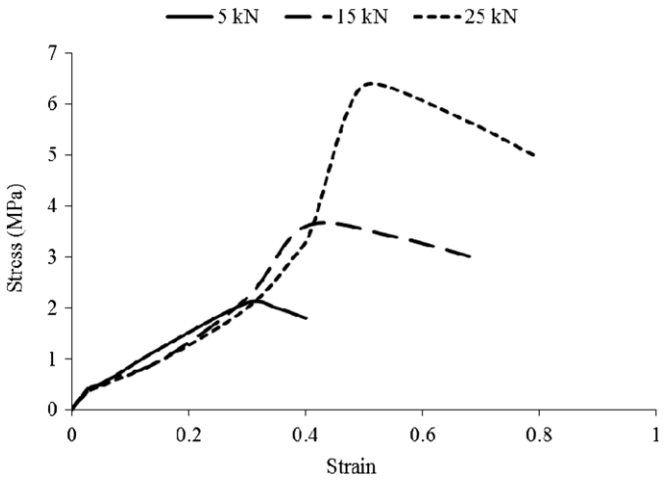

Figure 7. Stress–strain curve for different embossing forces.

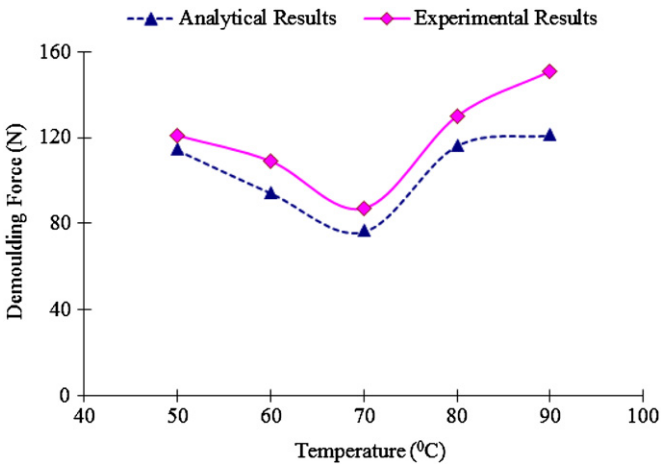

Figure 8. Comparison of experimental and analytical results as a function of the demoulding temperature.

5. Model implementation and validation

The analytical model presented earlier to predict the demoulding force, F_d, was implemented employing the Matlab software. The following sub-sections describe initial experiments conducted to obtain the necessary data to calculate the demoulding force with the proposed model as well as the experimental demoulding force measurements achieved to test its validity.

5.1. Adhesion and stress–strain tests

The adhesive energy at zero shrinkage strain, γ, defined by Kendall (1973) and that is required in equation (2) was assessed by embossing a flat mould with no structures onto a circular PMMA sheet. In particular, the demoulding force required was measured without cooling and thus, for a T_{dem} value of 150 °C. This force was assumed to include only the adhesion force component without any contributions from friction and deformation. Thus, based on equation (2) and by measuring the diameter and the thickness of the replica, γ was calculated to be equal to 13×10^{-3} J m^{-2}.

Stress–strain tests were also conducted for different embossing loads at 150 °C as shown in figure 7. These tests were important to measure the final thickness and diameter of the embossed PMMA sheets that are required for the proposed model. The strain rate of the material was calculated by measuring the cross bar movement of the embossing machine.

5.2. Effect of the embossing temperature on the demoulding force

The relationship between the demoulding temperature and the demoulding force is shown in figure 8. More specifically, this figure provides a comparison between the results obtained experimentally and those predicted by the analytical model for a range of demoulding temperatures and when considering the design with the structures located in the central area of the mould. Equation (1) was used to calculate the demoulding force F_d, and it particular, its value represents the sum of

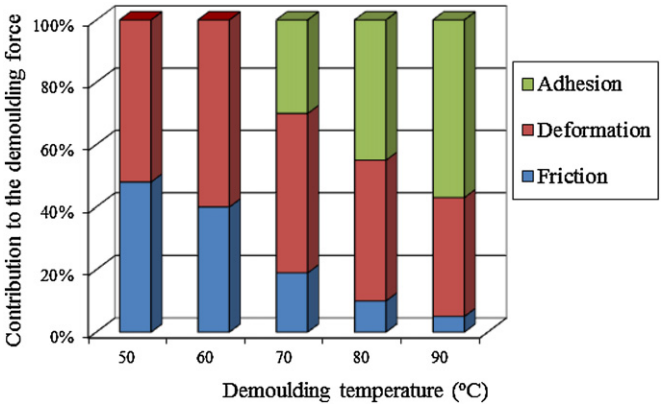

Figure 9. Percentage contribution of the phenomena considered in the model at different values of demoulding temperature.

the contributions from F_{ad}, described in equation (4), F_{def}, described in equation (5) and F_{fr}, described in equation (8). From this figure, it can be observed that the predicted values agree well with the experimental results with an average error of 13%. The demoulding force decreases initially as the demoulding temperature is reduced until it reaches a minimum value, and then it increases, which is in-line with studies reported earlier. The initial force reduction is due to the decrease in the adhesion force with the reduction of the demoulding temperature. However, the further reduction of the temperature leads to an increase of the friction force component as it becomes more dominant, which is also illustrated with the results given in figure 9. The variation of the deformation force is marginal and, according to equation (5), it is only influenced by the different values of the Young' modulus for PMMA for the range of temperature considered.

It can be seen from figure 8 that the analytical results underestimate the experimental demoulding force across the range of demoulding temperatures studied. This should be due to the fact that the model considers the pressure to be constant within the polymer during embossing while, in reality, it decreases during the holding stage of the process due to the creep time effect of the material. As a result, the pressure

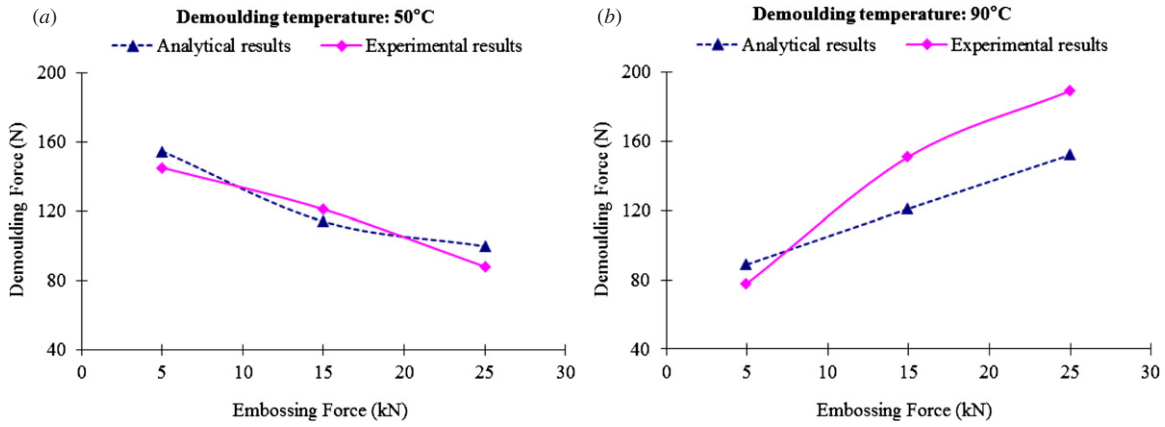

Figure 10. Comparison of experimental and analytical results for different embossing loads when demoulding at (*a*) 50 °C and (*b*) 90 °C.

value used in the model is larger than the experimental one, which in turn, leads to the underestimation of the friction force. In addition, it is noticed that the larger difference between the analytical and the experimental results occur for the higher demoulding temperature of 90 °C. This suggests that the calculated contribution of the adhesion force is less accurate at higher temperature. This result could be explained by the fact that, as described earlier, the implementation of the adhesion force model relies on initial experimental data to assess the thickness and diameter of embossed replicas without any contributions from the friction and deformation phenomena. However, such data were obtained by measuring the displacement of the cross bar of the HE machine and thus, there could be a larger degree of uncertainty associated with these measurements.

5.3. Effect of the embossing load on the demoulding force

In order to further test the capability of the proposed model, the comparison of experimental and analytical results for a range of embossing forces within the respective friction and adhesion dominated demoulding regimes is given in figure 10. The applied force generates different flow stresses and, the higher the applied pressure is, in regards to the yield point of the polymer, the less strain recovery is taking place. Also, a higher pressure within the polymer, caused by a higher embossing force, reduces the shrinkage effect, which in turn leads to a reduced contact stress on the sidewalls of the structures. At the same time, a high embossing load also reduces the final thickness of the replica and enlarges its area, which consequently leads to an increase of the adhesion force. These phenomena can be observed in figure 10. In particular, within the adhesion-dominated demoulding regime, i.e. at 90 °C, the lowest demoulding force is achieved with the lowest embossing load of 5 kN. This is due to the resulting smaller contact area and the reduced polymer shrinkage at this temperature. In contrast, in the friction-dominated regime, i.e. at 50 °C, a higher embossing load of 25 kN is required to achieve the lowest demoulding force. This can be explained with the fact that the higher pressure generated in the replica opposes the shrinkage effect. Again, a good agreement was achieved between the analytical and experimental results with

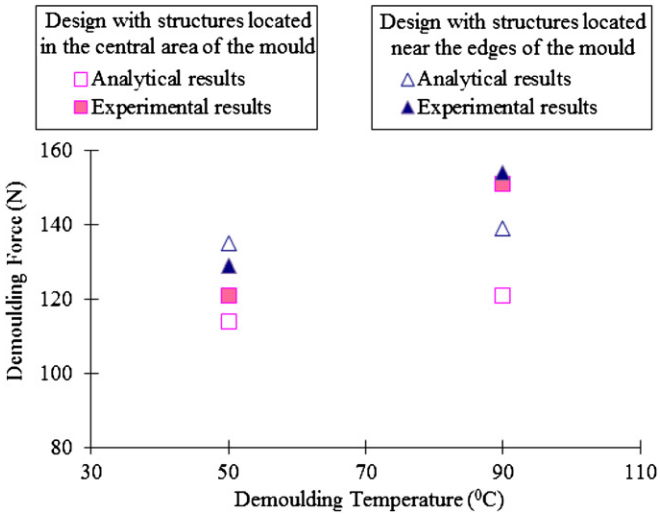

Figure 11. Comparison of experimental and analytical results for the structures located in the centre and near the edges of the mould.

a combined average prediction error of 15%. The larger error between the analytical and experimental results observed in the adhesion-dominated regime at higher embossing loads (see figure 10(*b*)) further supports the assumption put forward earlier that such discrepancies should be due to the less accurate experimental implementation of the adhesion force model adopted.

5.4. Effect of the mould design on the demoulding force

It can be seen in figure 11 that the demoulding force is higher, at both adhesion and friction dominant temperatures, for the design that incorporate structures located near the edge of the mould. The main reason for this difference is due to the fact that the thermal stress is higher at the edges.

6. Conclusions

This paper presents an analytical model to predict the required demoulding force in hot embossing. The distinguishing characteristic of the proposed model lies in integrating the contributions from the adhesion, friction and deformation

phenomena that take place when demoulding polymer microstructures. The close agreement between the analytical and experimental results confirms that the model describes successfully the relationships between the location and geometry of the mould structures, the pressure history in the polymer, the material properties, the demoulding temperature and the adhesion phenomenon on the resulting demoulding force. This study also confirmed that the layout of the mould structures has an effect on the required demoulding force. In addition, the applied load during the embossing stage of the process has a significant influence on demoulding. In particular, the pressure increase within the replica leads to raising the adhesion force due to the resulting higher contact area between the mould and the polymer while it also reduces the friction force due to the consequent decrease in the influence of the thermal stress.

Generally, it can be concluded that the developed model provides a valuable insight into the mechanisms that determine the demoulding force in HE by taking into account the effects and interdependences of the whole range of factors influencing the process. In addition, the model can be also used as a tool to optimize the demoulding stage of the HE process without the need for extensive experimental trials. Future work should focus on refining the model by considering the pressure change inside the polymer during holding time as well as the variation of the stress in the vertical direction and the evolution of the contact area between the mould and the polymer due to shrinkage.

Acknowledgments

The reported research was funded by the Engineering and Physical Sciences Research Council (ESPRC) under the grant EP/F056745/1 and the EC FP7 projects 'POLARIC' and 'IMPRESS'. The authors are also thankful for the financial support provided by the Ministry of Education of the Azerbaijan Republic.

References

Bhushan B 2003 Adhesion and stiction: mechanisms, measurement techniques, and methods for reduction *J. Vac. Sci. Technol.* B **21** 2262–96

Colton J S, Crawford J, Pham G, Rodet V and Wang K K 2001 Failure of rapid prototype molds during injection molding *CIRP Ann.* **50** 129–32

Delaney K, Bissacco G and Kennedy D 2010 A study of demoulding force prediction applied to periodic mould surface profiles *ANTEC'10: Society of Plastics Engineers Annu. Technical Conf.* pp 1279–84

Derjaguin B V, Muller V M and Toporov Y P 1975 Effect of contact deformations on the adhesion of particles *J. Colloid Interface Sci.* **53** 314–26

Dirckx M 2010 Demolding of hot embossed polymer microstructures *PhD Thesis* Mechanical Engineering, Massachusetts Institute of Technology, Cambridge, MA

Dirckx M and Hardt D E 2011 Analysis and characterization of demolding of hot embossed polymer microstructures *J. Micromech. Microeng.* **21** 1–10

Dirckx M, Taylor H K and Hardt D E 2007 High-temperature de-molding for cycle time reduction in hot embossing *ANTEC'07: Society of Plastics Engineers Annu. Technical Conf.* pp 2926–30

Elkaseer A M, Dimov S S, Popov K B, Negm M and Minev R 2012 Modeling the material microstructure effects on the surface generation process in microendmilling of dual-phase materials *J. Manuf. Sci. Eng.* **134** 044501

Esch M B, Kapur S, Irizarry G and Genova V 2003 Influence of master fabrication techniques on the characteristics of embossed microfluidic channels *Lab Chip* **3** 121–7

Gerberich W W and Cordill M J 2006 Physics of adhesion *Rep. Prog. Phys.* **69** 2157–203

Griffiths C A, Dimov S S, Scholz S, Hirshy H and Tosello G 2011 Process factors influence on cavity pressure behaviour on microinjection moulding *J. Manuf. Sci. Eng.* **133** 031007

Guo Y, Liu G, Xiong Y, Jun W, Xilong H and Tian Y 2007a Study of hot embossing using nickel and Ni-PTFE LIGA mold inserts *J. Microelectromech. Syst.* **16** 589–97

Guo Y, Liu G, Xiong Y and Tian Y 2007b Study of the demolding process—implications for thermal stress, adhesion and friction control *J. Micromech. Microeng.* **17** 9–19

Haisma J, Verheijein M, van den Heuvel K and van den Berg J 1996 Mold-assisted nanolithography: A process for reliable pattern replication *J. Vac. Sci. Technol.* B **14** 4124

Hansen H N, Hocken R J and Tosello G 2011 Replication of micro and nano surface geometries *CIRP Ann.* **60** 695–714

He Y, Fu J-Z and Chen Z-C 2005 Research on modeling of hot embossing polymeric microfluidic chip *J. Zhejiang Univ.* **39** 1911–4

Hirai Y, Yoshida S and Takagi N 2003 Defect analysis in thermal nanoimprint lithography *J. Vac. Sci. Technol.* B **21** 2765–70

Hsueh C-H, Lee S, Lin H-Y, Chen L-S and Wang W-H 2006 Analyses of mechanical failure in nanoimprint processes *Mater. Sci. Eng.* A **433** 316–22

Jaszewski R W, Schift H, Schnyder B, Schneuwly A and Gröning P 1999 The deposition of anti-adhesive ultra-thin teflon-like films and their interaction with polymers during hot embossing *Appl. Surf. Sci.* **143** 301–8

Johnson K L, Kendall K and Roberts A D 1971 Surface energy and the contact of elastic solids *Proc. R. Soc. Lond.* A **324** 301–13

Kendall K 1973 Shrinkage and peel strength of adhesive joints *J. Phys. D: Appl. Phys.* **6** 1782–7

Lin C-R, Chen R-H and Hung C 2003 Preventing non-uniform shrinkage in open-die hot embossing of PMMA microstructures *J. Mater. Process. Technol.* **140** 173–8

Menges G and Mohren P 1986 *How to Make Injection Moulds* (New York: Hanser)

Park S, Schift H, Padeste C, Schnyder B, Kötz R and Gobrecht J 2004 Anti-adhesive layers on nickel stamps for nanoimprint lithography *Microelectron. Eng.* **73–74** 196–201

Park S, Song Z, Brumfield L, Amirsadeghi A and Lee J 2009 Demolding temperature in thermal nanoimprint lithography *Appl. Phys.* A **97** 395–402

Pham G T and Colton J S 2002 Ejection force modeling for stereolithography injection molding tools *Polym. Eng. Sci.* **42** 681–93

Prokopovich P and Starov V 2011 Adhesion models: from single to multiple asperity contacts *Adv. Colloid Interface Sci.* **168** 210–22

Prokopovich P, Theodossiades S, Rahnejat H and Hodson D 2010 Nano- and component level scale friction of rubber seals in dispensing devices *Wear* **268** 845–52

Saha B, Liu E, Tor S B, Khun N W, Hardt D E and Chun J H 2010 Replication performance of Si-N-DLC-coated Si micro-molds in micro-hot-embossing *J. Micromech. Microeng.* **20** 045007

Song Z, Choi J, You B H, Lee J and Park S 2008 Simulation study on stress and deformation of polymeric patterns during the

demolding process in thermal imprint lithography *J. Vac. Sci. Technol.* B **26** 598–605
Titomanlio G and Jansen K M B 1996 In-mold shrinkage and stress prediction in injection molding *Polym. Eng. Sci.* **36** 2041–9
Trabadelo V, Schift H, Merino S, Bellini S and Gobrecht J 2008 Measurement of demolding forces in full wafer thermal nanoimprint *Microelectron. Eng.* **85** 907–9
Worgull M 2009 *Hot Embossing: Theory and Technology of Microreplication* (Oxford: Elsevier)
Worgull M and Heckele M 2004 New aspects of simulation in hot embossing *Microsyst. Technol.* **10** 432–7
Worgull M, Heckele M and Schomburg W K 2005 Large-scale hot embossing *Microsyst. Technol.* **12** 110–5
Worgull M, Hétu J-F, Kabanemi K K and Heckele M 2008a Hot embossing of microstructures: characterization of friction during demolding *Microsyst. Technol.* **14** 767–73
Worgull M, Kabanemi K K, Marcotte J-P, Hétu J-F and Heckele M 2008b Modeling of large area hot embossing *Microsyst. Technol.* **14** 1061–6